Thermodynamics of Zn²⁺ Binding to Cys₂His₂ and Cys₂HisCys Zinc Fingers and a Cys₄ Transcription Factor Site

Anne M. Rich,[†,∥] Elisa Bombarda,[‡,⊥] Austin D. Schenk,[†] Paul E. Lee,[†] Elizabeth H. Cox,[†] Anne M. Spuches,[†,⊗] Lynn D. Hudson,[§,▽] Bruno Kieffer,[#] and Dean E. Wilcox*,[†]

[†]Department of Chemistry, Dartmouth College, Hanover, New Hampshire 03755, United States

[‡]Laboratoire de Pharmacologie et Physio-Chimie des Interactions Cellulaires et Moléculaires, Université Louis Pasteur, 67401 Illkirch, France

[§]Section of Developmental Genetics, National Institute of Neurological Disorders and Stroke, Bethesda, Maryland 20892, United States

[#]Département de Biologie Structurale et Génomique, Institut de Génétique et de Biologie Moléculaire et Cellulaire, 67404 Illkirch, France

S Supporting Information

ABSTRACT: The thermodynamics of Zn²⁺ binding to three peptides corresponding to naturally occurring Zn-binding sequences in transcription factors have been quantified with isothermal titration calorimetry (ITC). These peptides, the third zinc finger of Sp1 (Sp1-3), the second zinc finger of myelin transcription factor 1 (MyT1-2), and the second Zn-binding sequence of the DNA-binding domain of glucocorticoid receptor (GR-2), bind Zn²⁺ with Cys₂His₂, Cys₂HisCys, and Cys₄ coordination, respectively. Circular dichroism confirms that Sp1-3 and MyT1-2 have considerable and negligible Zn-stabilized secondary structure, respectively, and

	Sp1-3 (C₂H₂)	MyT1-2 (C₂HC)	GR-2 (C₄)	
$\Delta G°$	-10.5 ± 0.3	-9.4 ± 0.4	-10 ± 1	kcal/mol
$\Delta H°$	-5.2 ± 0.2	-2 ± 1	+10 ± 2	kcal/mol
$-T\Delta S°$	-5.3 ± 0.2	-7.5 ± 1.5	-20 ± 2	kcal/mol

indicate only a small amount for GR-2. The pK_a's of the Sp1-3 cysteines and histidines were determined by NMR and used to estimate the number of protons displaced by Zn²⁺ at pH 7.4. ITC was also used to determine this number, and the two methods agree. Subtraction of buffer contributions to the calorimetric data reveals that all three peptides have a similar affinity for Zn²⁺, which has equal enthalpy and entropy components for Sp1-3 but is more enthalpically disfavored and entropically favored with increasing Cys ligands. The resulting enthalpy–entropy compensation originates from the Zn-Cys coordination, as subtraction of the cysteine deprotonation enthalpy results in a similar Zn²⁺-binding enthalpy for all three peptides, and the binding entropy tracks with the number of displaced protons. Metal and protein components of the binding enthalpy and entropy have been estimated. While dominated by Zn²⁺ coordination to the cysteines and histidines, other residues in the sequence affect the protein contributions that modulate the stability of these motifs.
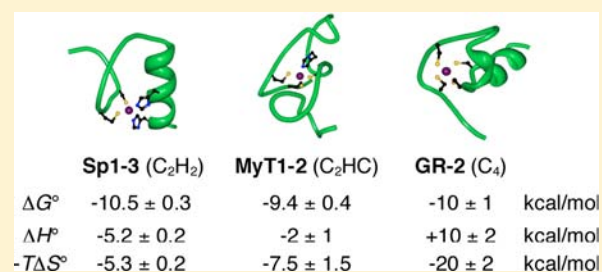
INTRODUCTION

Many transcription factors that regulate gene expression require one or more Zn²⁺ ions to stabilize a protein structure for sequence-specific binding to DNA. Initially discovered in TFIIIA as tandem repeat sequences[1] known as zinc fingers,[2,3] which have been studied extensively as isolated peptides,[4] this motif consists of a short, antiparallel β sheet (reverse turn) containing two Zn-binding Cys residues, followed by an α helix containing two His residues that complete a Cys₂His₂ tetrahedral Zn²⁺ coordination.[5,6] This ββα motif also has three conserved hydrophobic residues that form a small hydrophobic core and thus many of the features of a metal-stabilized globular domain.

Several other Zn-binding motifs with Cys and His residues and a variety of Zn-stabilized structures have been found,[7] although the initial (classical) zinc finger is the most common in eukaryotic transcription factors. Notable are the two Zn-binding sequences of the retroviral nucleocapsid protein, which

provide Cys₂HisCys coordination for the Zn²⁺.[8] Another well-characterized Zn-stabilized motif is the ~90 residue DNA-binding domain of glucocorticoid receptor (GR-DBD),[9] which is similar to that of other members of the hormone receptor family. Tetrahedral coordination of two Zn²⁺ ions to four different Cys residues in this domain stabilizes a structure[10] that makes both protein−DNA contacts (first Zn-binding sequence) and protein−protein contacts (second Zn-binding sequence) when GR binds as a dimer to its DNA recognition sequence.[11] Peptides corresponding to these two Zn-binding sequences of GR-DBD[12] and the DNA-binding domain of estrogen receptor (ER-DBD)[13] have been studied. Thus, different combinations of Cys and His residues are used for Zn²⁺ coordination and stabilization of protein structures.

Despite numerous studies of zinc finger peptides and Zn-stabilized domains, questions remain about metal coordination to these protein motifs. First, the relative thermodynamic contributions of metal coordination and protein interactions (e.g., hydrogen bonding of α helix and β sheet) to the overall stability are not well understood. Second, modulation of Zn^{2+} availability and reversible stabilization of these DNA-binding structures has been proposed as a mechanism for regulating transcription.[14,15] Third, these Zn-binding sites may be targets for certain toxic metals[16] that can displace the Zn^{2+} and alter the protein structure or cleave the protein,[17] thereby compromising gene expression and disrupting biochemical pathways.

These biophysical, biochemical, and toxicological questions require quantitative measurements of the thermodynamics of metal ions binding to these sites, and the technique of isothermal titration calorimetry (ITC) is capable of this task.[18] In many cases a complete thermodynamic analysis can be obtained in a single experiment, and the binding of different metal ions, including spectroscopically challenging Zn^{2+}, can be studied directly under identical conditions.

Previous studies have used ITC to quantify metal binding to zinc finger peptides. One of the first measured the enthalpy of Zn^{2+} binding to a short peptide corresponding to one of the $Cys_2HisCys$ Zn-binding sites of the HIV-1 nucleocapsid protein.[19] A pair of studies measured Zn^{2+} binding to a classical Cys_2His_2 zinc finger and its variants with alternate residues to determine the thermodynamic consequences of these substitutions.[20,21] Blaise and Berg used ITC to quantify the enthalpy of Co^{2+} and Zn^{2+} binding to the optimized "consensus" zinc finger, CP-1,[22] to compare the thermodynamics and evaluate the entropic factors in metal stabilization of the protein structure.[23] Subsequently, Weiss and co-workers used a number of physical methods, including ITC, to evaluate the enthalpic contributions to Co^{2+} and Zn^{2+} binding to zinc fingers.[24] Finally, Gibney and co-workers prepared a series of short glycine-rich peptides (designated GGG) that contain four Cys/His residues and quantified their Zn-binding thermodynamics with ITC and other methods.[25]

Earlier we reported a critical analysis of the use of ITC to quantify metal binding to peptides and proteins,[26] and recently we summarized further insight into a set of guidelines for experimental conditions and data analysis.[27] The overall equilibrium in eq 1 summarizes Zn^{2+} binding to these peptides:

$$Zn(buffer)_m^{2+} + peptide^{p+} + (n-m)buffer$$
$$\rightleftharpoons Zn(peptide)^{(p+2-n)+} + n(bufferH^+) \qquad (1)$$
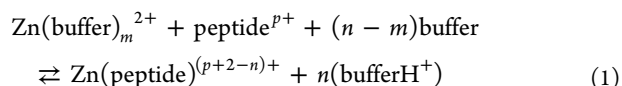
Both proton displacement and metal−buffer interactions must be considered to determine accurate condition-independent stability constants and thermodynamic values. Based on this insight, we have now used ITC to quantify the thermodynamics of Zn^{2+} binding to peptides corresponding to three naturally occurring Zn-binding sequences in transcription factor proteins.

Studied in most detail was a peptide corresponding to the third zinc finger from the DNA-binding domain of the transcription factor Sp1,[28] designated Sp1-3. As predicted from its sequence, which conforms to the canonical pattern of zinc finger residues ($F/YXCX_{2-4}CX_3FX_5LX_2HX_3H$, where X = variable residues), and confirmed by NMR spectroscopy,[29] this peptide adopts the structure of a classical Cys_2His_2 zinc finger upon binding Zn^{2+} (Figure 1). Its metal-binding properties

have been investigated previously with spectroscopic methods.[30]
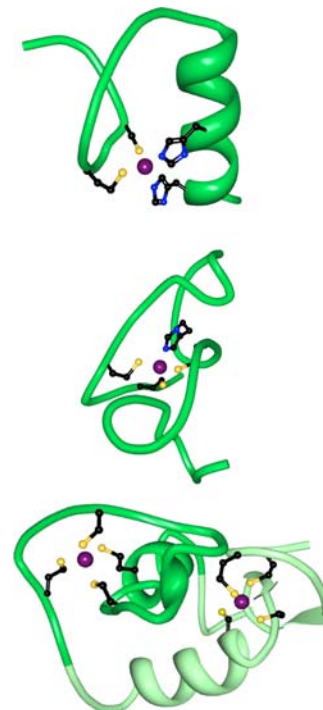

Figure 1. Peptide ribbon diagrams and Zn^{2+}-coordinating side chains for (top) Sp1-3 (PDB 1SP2), (middle) NZF-1 (PDB 1PXE), and (bottom) GR-DBD (PDB 2GDA), with the GR-2 ribbon highlighted for the latter.

Also studied was a peptide corresponding to the second zinc finger from the human myelin transcription factor 1,[31] designated MyT1-2, which is representative of a class of sequences with conserved Cys and His residues ($CX_4CX_4HX_7HX_5C$) similar to that of the canonical zinc finger. A closely related peptide (93% identical) from the rat Neural Zinc Finger Factor 1 (NZF-1)[32] binds Co^{2+} with $Cys_2HisCys$ coordination through either of the two conserved His residues.[33] An NMR structure of a somewhat longer NZF-1 peptide (Figure 1) confirmed the expected $Cys_2HisCys$ coordination of Zn^{2+} and showed an absence of the secondary structure found with classical zinc fingers.[34] This was confirmed by the NMR structure of a peptide corresponding to the fifth zinc finger of the mouse MyT1.[35]

The final peptide in this study corresponds to the second Zn-binding sequence in the DNA-binding domain of glucocorticoid receptor (GR-DBD), designated GR-2,[12] which has a sequence of Cys residues ($CX_5CX_9CX_2CX_4C$) that is conserved among the hormone receptors. While the NMR structure of the whole domain[10] shows that this Zn^{2+} stabilizes some α helices (Figure 1), the structure of the independent peptide is not known, though its CD spectrum indicates little Zn-stabilized secondary structure.[12]

The calorimetric studies described herein provide novel insight about Zn^{2+} binding to different coordination sites in transcription factor proteins. First, we find that Zn^{2+} displaces the proton from each coordinated Cys residue, further refuting the notion that Cys thiols in peptides such as these and corresponding proteins remain protonated upon Zn^{2+} coordination in aqueous solution. Second, the Zn^{2+}-binding constants

obtained from direct ITC measurements are compared to those determined from spectrophotometric measurements, which use indirect Co^{2+} displacement to study spectroscopically silent Zn^{2+}. Third, the thermodynamics of Zn^{2+} binding to these naturally occurring sequences have been quantified. All three bind Zn^{2+} with a similar affinity, but this is equally enthalpically and entropically favored for this classical Cys_2His_2 zinc finger, less enthalpically favored and more entropically driven for the $Cys_2HisCys$ coordination of MyT1-2, and an entropically driven binding for the Cys_4 coordination of GR-2. Finally, we have estimated the metal and protein contributions to the overall binding thermodynamics and find that the metal coordination dominates, though other residues modulate the enthalpic and entropic contributions from the protein to the overall stability.

■ EXPERIMENTAL SECTION

All reagents were obtained from Sigma and were ≥99% pure. Stock solutions of Zn^{2+} and Co^{2+} were prepared from $ZnSO_4 \cdot 7H_2O$ or $ZnCl_2$ and $CoCl_2$. Buffer solutions were made with nanopure (>18 MΩ resistance) water and treated with Chelex-100 resin to remove trace metals prior to their use in preparing peptide and metal solutions. The 27-residue human Sp1-3 peptide, KFA**C**PE**C**PKRFMRSDHLS-K**H**IKT**H**QNK, the 29-residue human MyT1-2 peptide, LK**C**PTPG**C**TGQGHVNSNRNT**H**RSLSG**C**PI, its analogue with Gln replacing the His at position 13, and the 31-residue capped (N-acetylated and C-amidated) and uncapped rat GR-2 peptide, YL**C**AGRND**C**IIDKIRRKN**C**PA**C**RYRKCLQAG (bold residues are known or putative Zn-coordinating residues), were synthesized by solid-phase peptide synthesis at the HHMI Biopolymer/Keck Foundation Biotechnology Resource Laboratory at Yale University. The peptides were reduced with excess dithiothreitol (DTT), purified by reverse-phase HPLC on a Ranin HPXL system with a Vydac C-18 semipreparative column, lyophilized, and stored at −80 °C. Their identity was verified by MALDI-MS (Sp1-3, m/z = 3269.4 (3267.9 expected); MyT1-2, m/z = 3036.7 (3035.5 expected); GR-2, m/z = 3640.8 (3643.4 expected)) at the Molecular Biology Core Facility of the Dartmouth Medical School, and their purity was determined to be ≥95% by reverse-phase HPLC with a Vydac C-18 analytical column.

Peptide concentrations were determined with a 5,5′-dithio-bis(2-nitrobenzoic acid) (DTNB) assay (ε_{412nm} = 14 150 M^{-1} cm^{-1}) for reduced Cys.[36] The GR-2 concentration was also determined by the absorbance of its two Tyr residues at 274 nm (ε_{274nm} = 2680 M^{-1} cm^{-1}). UV−vis absorption measurements of metal ion titrations were obtained at ambient temperature with a PerkinElmer λ-9 spectrophotometer. Solutions were deoxygenated with N_2 or Ar gas and kept under an inert atmosphere in sealed quartz cuvettes. Spectral data of metal titrations were analyzed with commercially available Specfit software.[37] A JASCO J-715 spectropolarimeter was used to obtain CD measurements at ambient temperature under anaerobic conditions.

For ^1H NMR measurements, 2 mg of Sp1-3 was dissolved in 500 μL of H_2O with 10 mM deuterated DTT and 0.1 M NaCl to a final concentration of ~1 mM. Next, 30 μL of ^2H_2O was added to provide a signal to lock the spectrometer field, and Ar was bubbled through the solution to create anaerobic conditions. All spectra were recorded on Bruker DRX 500 and DRX 600 spectrometers. The spectral width was set to 10 ppm in both dimensions, and 512 t_1-increments of 2048 points were used. Water suppression was achieved by a WATERGATE sequence.[38,39] The peptide resonance assignments were based on two-dimensional phase-sensitive HOHAHA[40,41] (80 ms mixing times) and NOESY[42] (600 ms mixing times) spectra. Two sets of assignments were obtained for each of the conditions, pH 3.7 at 288 K and pH 6.6 at 283 K.

The NMR data were processed with Bruker XWIN NMR software. Sine bell window functions were used for apodization prior to Fourier transformation in both dimensions, with a final matrix size of 2048 × 1024. The set of spectra at pH 3.7 and 288 K that was used for the initial assignments was referenced to an external 3-(trimethylsilyl)-1-

propanesulfonic acid (DSS) signal. The pK_a's of titratable groups were determined by monitoring chemical shifts of the relevant protons on two-dimensional HOHAHA spectra recorded at 298 K. A total of 25 measurements were recorded at pH values ranging from 3.7 to 10.5. The pH was adjusted by adding small amounts of 100 mM NaOH or 100 mM HCl and measured with a thin Beckman pH electrode inserted directly into the NMR tube; the pH was determined before and after each set of NMR experiments and never varied by more than 0.15 pH unit. The NMR tube was opened under an argon flow to maintain anaerobic conditions. To confirm reversibility of the titration, after the highest pH spectrum was obtained, the pH was adjusted back to 4.0, and this spectrum was compared to the original pH 4.0 spectrum.

Isothermal titration calorimetry measurements were obtained at 25 ± 0.2 °C as described previously[26] with a MicroCal MCS titration microcalorimeter located inside a custom-built plexiglass glovebox filled with nitrogen to maintain an inert atmosphere. The data were analyzed with a one-site binding model or a competition binding model[43] by the Origin software package supplied by MicroCal. The stirring speed was typically 300 or 500 rpm, and sufficient time was allowed between injections to reach equilibrium (baseline). Multiple ITC measurements were made for each type of experiment, and quantitative results are the average of the best-fit parameter from at least two and typically three or more consistent data sets. The ITC data are presented by showing the baseline-adjusted experimental titration (heat flow versus time) on the top and the peak-integrated concentration-normalized molar heat flow per aliquot versus the titrant-to-sample molar ratio on the bottom. The solid line in the bottom plot represents the best fit of the data to the one-site equilibrium binding expression. The average best-fit values were analyzed, as described previously,[27] to account for the contributions of metal−buffer interaction to the experimental binding constant, and metal−buffer and buffer protonation enthalpies to the experimental binding enthalpy.

■ RESULTS AND ANALYSIS

Spectrophotometry. All three peptides bind Co^{2+} with ~T_d coordination, indicated by the intensities and energies of their ligand field spectra in the 12 000−19 000 cm^{-1} region (Figure 2), which is assigned as the $^4A_1$-to-$^4T_1(P)$ transition split by low symmetry at the peptide site.[44] The progressive red shift of the envelope of ligand field transitions from Sp1-3 to MyT1-2 to GR-2 is consistent with the expected substitution of the harder His imidazole by the softer Cys thiolate, as reported for CP-1 and its variants with Cys_2His_2, Cys_3His, and Cys_4 coordination.[45]
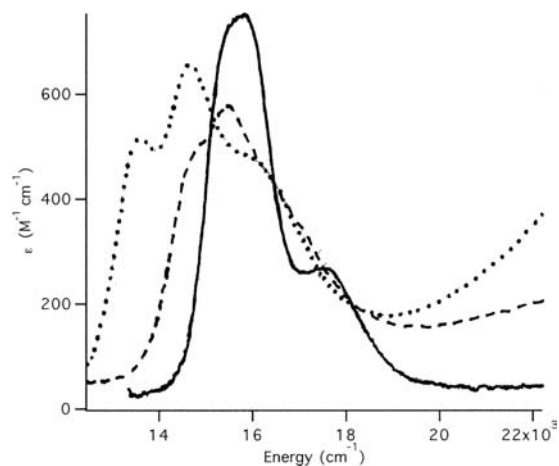

Figure 2. Visible and near-IR absorption spectra of the Co^{2+} complex of Sp1-3 (—), MyT1-2 (---) and GR-2 (···).

The Zn^{2+} affinity of the three peptides was initially quantified by spectrophotometrically monitoring the binding of Co^{2+} and then its displacement by Zn^{2+} under anaerobic conditions.

The UV−vis titrations for Sp1-3 were reported earlier, and nonlinear least-squares analysis at a single wavelength gave $K_{Co} = (3 \pm 1) \times 10^6$ and $K_{Zn} = (2 \pm 1) \times 10^9$ at pH 7.0 (50 mM HEPES, 50 mM NaCl).[30] These spectral data (Figure 3B,C in ref 24) have now been analyzed with the Specfit multiple-wavelength nonlinear least-squares fitting algorithm, and the binding constants with this improved fitting analysis are found to be $(1.0 \pm 0.1) \times 10^6$ for Co^{2+} and $(1.0 \pm 0.1) \times 10^8$ for Zn^{2+}. Accounting for buffer competition ($\log K_{Co\text{-HEPES}} = 3.25$; $\log K_{Zn\text{-HEPES}} = 3.38$) at this pH and buffer concentration[27] gives buffer-independent values of $(3 \pm 1) \times 10^7$ for Co^{2+} and $(4 \pm 1) \times 10^9$ for Zn^{2+}.

The UV−vis absorption spectrum of Co^{2+} bound to MyT1-2 is similar to that reported for a peptide (NZF-13) corresponding to a closely related Zn-binding sequence of the transcription factor NZF-1.[33] Specfit analysis of Co^{2+} and Zn^{2+} spectral titration data (Figure S1 of Supporting Information) at pH 7.0 (50 mM HEPES, 50 mM NaCl) gives the binding constants $(2.0 \pm 0.5) \times 10^5$ for Co^{2+} and $(4 \pm 1) \times 10^7$ for Zn^{2+}. Accounting for metal−buffer interaction, as indicated above, gives buffer-independent values of $(5.0 \pm 0.5) \times 10^6$ for Co^{2+} and $(1.0 \pm 0.1) \times 10^9$ for Zn^{2+}.

The UV−vis absorption spectra of both capped and uncapped GR-2 titrated with Co^{2+} and subsequently back-titrated with Zn^{2+} consistently showed that the latter titration does not result in the spectrum of a fresh GR-2 sample with 1 equiv of Zn^{2+} (Figure S2 of Supporting Information). We attribute this to contributions from the absorption of displaced Co^{2+} that remains bound to the conserved fifth Cys residue, light scattering and/or disulfide absorption from peptide that becomes oxidized during the titration due to its five Cys residues, and some absorption from oxidized Co^{3+} ions (weak features at 390 and 470 nm). Thus, any binding constants obtained from fitting these data are not reliable.

The amount of secondary structure that is stabilized by Zn^{2+} coordination to each peptide was investigated by their CD spectra in the 180−280 nm range (Figure 3). The Sp1-3 CD spectra reported earlier[30] were only accurate for $\lambda > 200$ nm, and the large positive feature at ~190 nm reported here is consistent with the Zn-stabilized α helix and β sheet that were determined by NMR spectroscopy.[29] The UV CD data for MyT1-2 indicate that Zn^{2+} does not stabilize secondary structure, consistent with the NMR structure of a related NZF-1 peptide[34] and the fifth zinc finger of mouse MyT1.[35] Since this sequence has another conserved His that could coordinate the Zn^{2+} and stabilize an alternative protein structure, a variant with Gln replacing the His in position 13 (MyT1-2(H13Q)) was prepared and found to have nearly identical UV CD spectra (Figure S3 of Supporting Information), indicating $Cys_2HisCys$ coordination with His-21 in the native sequence. Finally, the UV CD spectra of GR-2 in the absence and presence of Zn^{2+} are very similar to those reported previously[12] and indicate that only a small amount of secondary structure is stabilized by Zn^{2+} coordination to this peptide.

NMR Spectroscopy. A complete thermodynamic analysis of metal ions binding to proteins and peptides requires quantitative information about the acid/base properties of the residues that coordinate the metal. As described previously,[46] NMR spectroscopy was used to determine the pK_a's of the
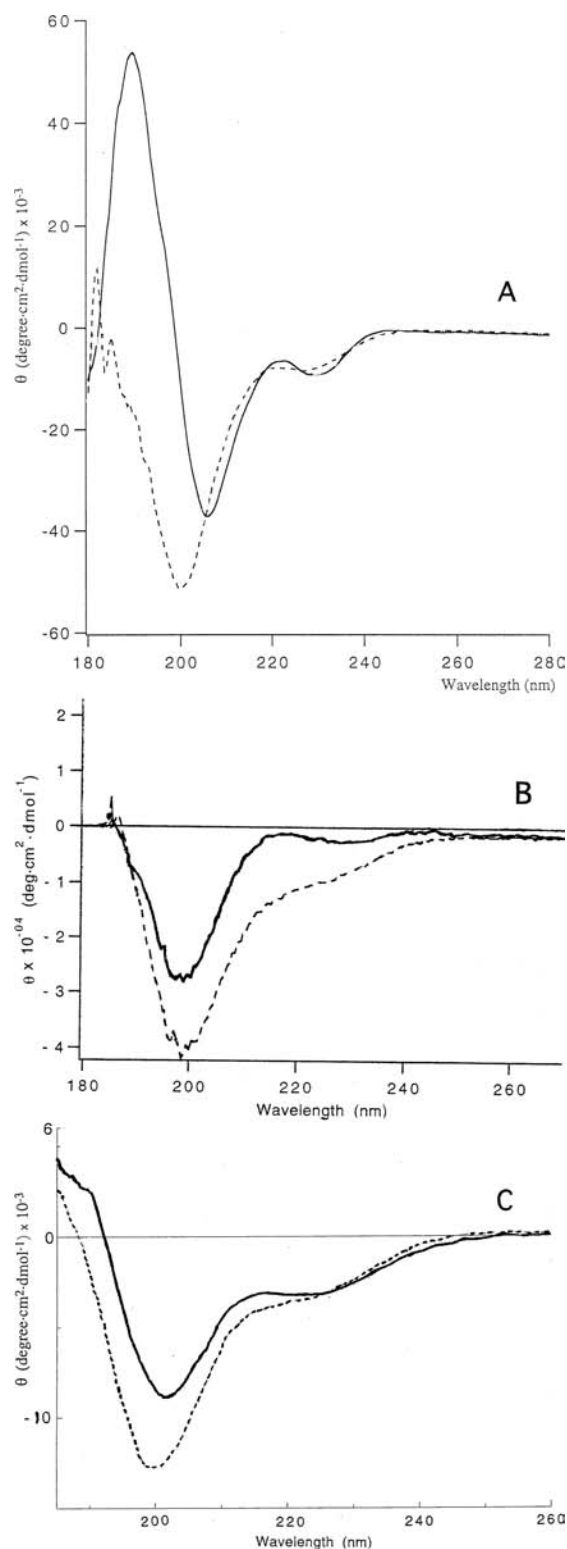

Figure 3. UV CD spectra of the apo peptide (---) and Zn^{2+} complex (—) of (A) Sp1-3, (B) MyT1-2, and (C) GR-2. Spectra were collected at ambient temperature in 10 mM phosphate buffer, pH 7.0, with 1.2−1.3 equiv of metal.

metal-binding His and Cys residues of the Sp1-3 peptide, which differs slightly in its N- and C-terminal residues from the peptide whose structure was determined by NMR methods.[29] The ^1H NMR resonances of Sp1-3 were first assigned at pH 3.7 using the procedure described by Wüthrich[47] (Figure 4). The
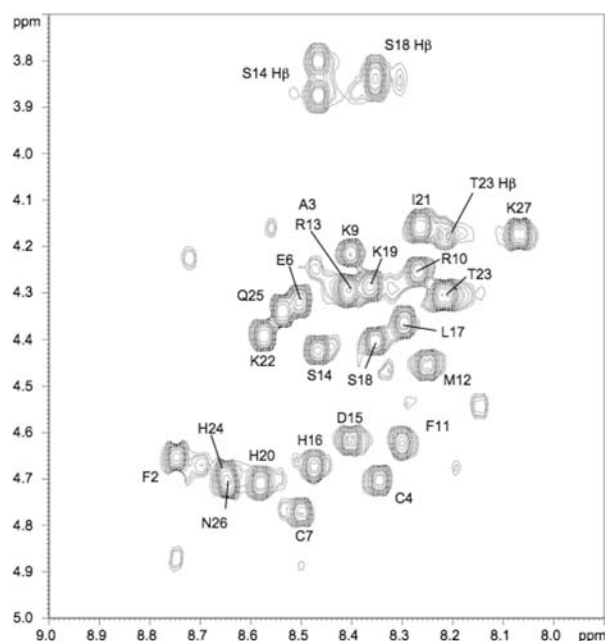
Figure 4. A portion of the HOHAHA spectrum of Sp1-3 (80 ms mixing time, pH 3.7, 288 K) showing backbone assignments.

poor spectral dispersion of the amide protons, together with the absence of medium-range NOEs, showed that the peptide was not folded in the absence of Zn^{2+}. The protonation state of each Cys residue was monitored by the chemical shift of its H^β proton resonances using H^α–H^β cross-peaks in the HOHAHA spectrum (Figure 5A). Similarly, the correlation between $H^{\delta2}$ and $H^{\varepsilon1}$ of imidazoles in the aromatic region of the HOHAHA spectrum was used to monitor protonation of the three His residues (Figure 5B). Despite very similar chemical shifts, the resolution of the 2D spectra allowed the three His aromatic spin systems to be distinguished. The chemical shifts of the $H^{\varepsilon1}$ and $H^{\delta2}$ His resonances change by ~0.9 and ~0.3 ppm, respectively, suggesting that the major tautomeric form has a protonated $N^{\varepsilon2}$. In contrast, the H^β resonances of the Cys residues change by only ~0.1 ppm upon deprotonation of the thiol side chain. Moreover, the shift induced by thiol deprotonation leads to spectral overlap for the H^α–H^β

correlation between pH 7 and 8, resulting in larger uncertainties for the pK_a values of the Cys4 and Cys7 thiols.

The pH dependence of the chemical shift of the aromatic His protons could be fitted adequately with eq 2,[46] where δ is the

$$\delta = \frac{\delta_{max} + \delta_{min}10^{pH-pK_a}}{1 + 10^{pH-pK_a}} \qquad (2)$$

chemical shift at a given pH, and δ_{max} and δ_{min} are the chemical shifts of the acidic and basic forms, respectively (Figure 6A–C). The pK_a values determined for these His residues (Table 1) are typical for solvent-exposed histidines.[48]

The pK_a's of the two Cys residues were determined by fitting the pH dependence of the thiol methylene chemical shifts. In the case of Cys4, the two H^β protons were resolved (Figure 6D), and the pH dependence of both H^β resonances is well fitted to a single pK_a with eq 2 (Table 1). In the case of Cys7, the two H^β signals were not resolved. Interestingly, the pH profile of these methylene protons indicates that two protonations affect their chemical shift (Figure 6E). A good fit of the experimental data is obtained with eq 3,[46] which

$$\delta = \frac{\delta_0 + \delta_1 10^{pH-pK_{a1}} + \delta_2 10^{2pH-pK_{a1}-pK_{a2}}}{1 + 10^{pH-pK_{a1}} + 10^{2pH-pK_{a1}-pK_{a2}}} \qquad (3)$$

assumes a sequential titration of two non-interacting acidic groups, where δ_0, δ_1, and δ_2 are the chemical shifts of the acidic, intermediate, and basic forms, respectively. The two pK_a values are determined to be 4.4 ± 0.4 and 8.2 ± 0.2, with the higher one identified as that of the Cys7 thiol. The presence of an additional titratable group in the acidic range suggests that the H^β protons of Cys7 are sensitive to the protonation state of the carboxylate of the adjacent Glu6. To test this, the pH dependence of the chemical shift of the H^γ of Glu6 was determined. The fit of these experimental points to eq 2 yields a pK_a of 4.3 ± 0.4 (Figure 6F), confirming this assumption.[49]

Calorimetry. ITC was used to quantify the thermodynamics of Zn^{2+} binding to the naturally occurring sequences of the Sp1-3, MyT1-2, and GR-2 peptides under anaerobic conditions. A survey of the effect of pH and buffer on the Sp1-3 data led to an optimal pH, which is based on three factors. First, the pK_a's
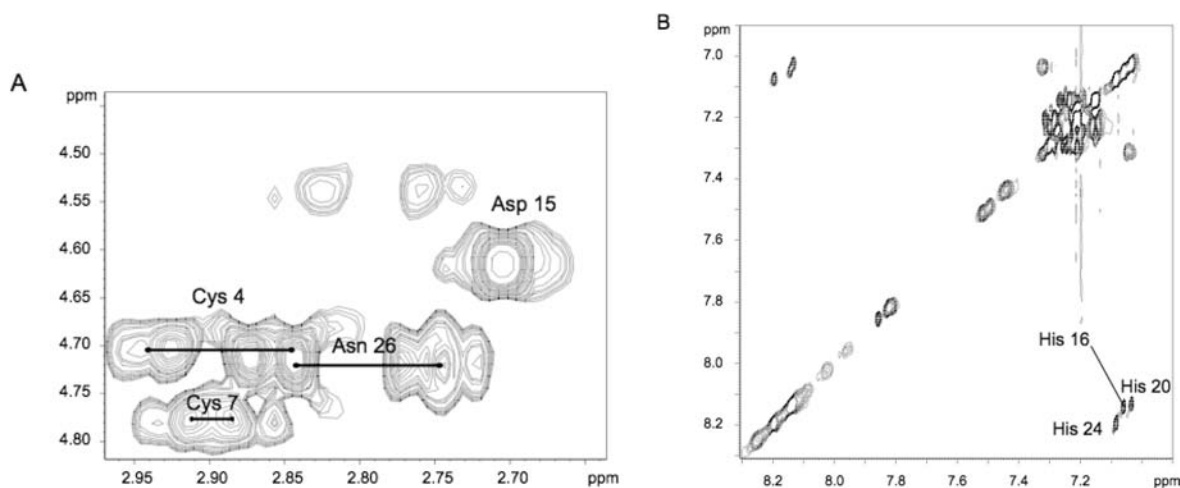

Figure 5. A portion of the HOHAHA spectrum of Sp1-3 showing (A) Cys H^β assignments (80 ms mixing time, pH 3.7, 288 K) and (B) His $H^{\varepsilon1}$ and $H^{\delta2}$ assignments (40 ms mixing time, pH 6.0, 298 K).
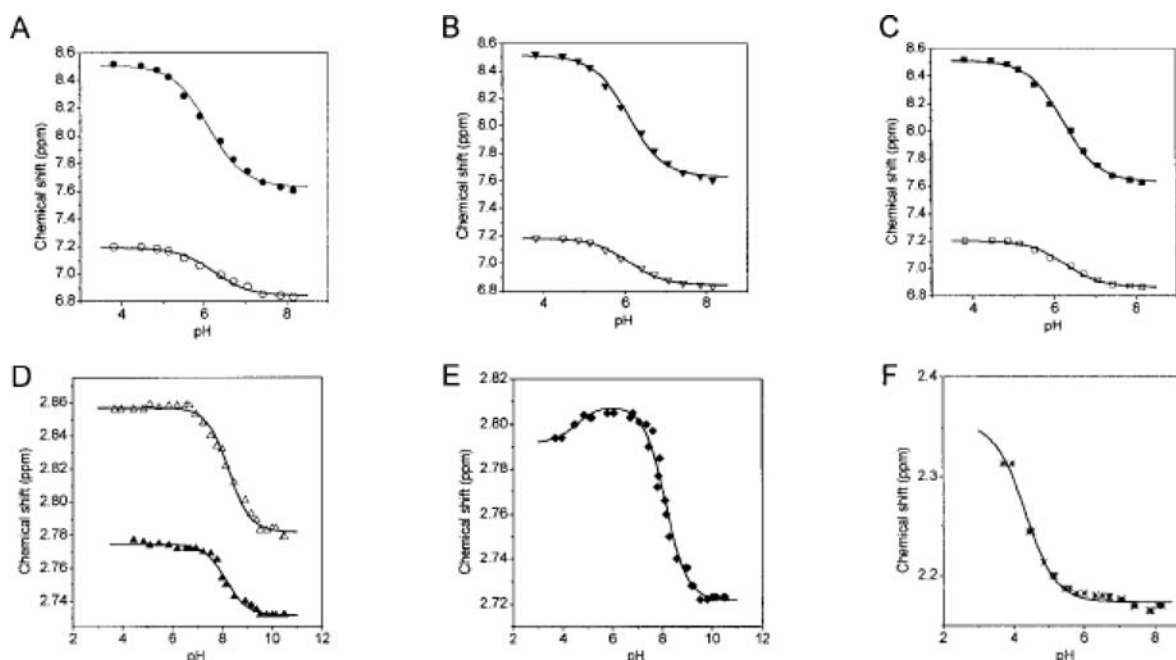
Figure 6. Plots of the pH dependence of the chemical shift: (A) $H^{\delta 2}$ (open) and $H^{\varepsilon 1}$ (solid) of the imidazole ring of His16; (B) $H^{\delta 2}$ (open) and $H^{\varepsilon 1}$ (solid) of the imidazole ring of His20; (C) $H^{\delta 2}$ (open) and $H^{\varepsilon 1}$ (solid) of the imidazole ring of His24; (D) $H^{\beta 1}$ (open) and $H^{\beta 2}$ (solid) of Cys4; (E) H^{β} protons of Cys7; and (F) H^{γ} protons of Glu6. Continuous lines are the fits to eq 2, except for (E), which is the fit to eq 3; the best-fit pK_a values are found in Table 1.

Table 1. pK_a Values of Selected Sp1-3 Residues Determined by ^{1}H NMR at 25 °C

residue		pK_a
His16	$H^{\delta 2}$, $H^{\varepsilon 1}$	6.2 ± 0.1
His20	$H^{\delta 2}$, $H^{\varepsilon 1}$	6.1 ± 0.1
His24	$H^{\delta 2}$, $H^{\varepsilon 1}$	6.2 ± 0.1
Cys4	$H^{\beta 1}$ [a]	8.3 ± 0.2
	$H^{\beta 2}$ [a]	8.1 ± 0.2
Cys7	H^{β}	4.4 ± 0.4; 8.2 ± 0.2
Glu6	H^{γ}	4.3 ± 0.4

[a]The stereospecificity of these H^{β} methylene protons has not been assigned.

of the His and Cys residues determined by NMR spectroscopy (Table 1) indicate that Sp1-3 samples at pH 7.4 have predominantly unprotonated (neutral) His imidazoles and protonated (neutral) Cys thiols, and the same is expected for MyT1-2 and GR-2 at this pH. Second, pH 7.4 is within the useful buffering range for Tris, which has a large heat of protonation and a relatively well characterized, and thus easily subtracted, interaction with metal ions. Finally, although we hoped to include data at different pH's, isotherms of Zn^{2+} binding to Sp1-3 at pH 7.8 in HEPES buffer contained a second thermodynamic event that may be due to hydrolysis chemistry at higher pH in this buffer.

Representative ITC data for Zn^{2+} binding to Sp1-3, MyT1-2, and GR-2 at pH 7.4 in 20 mM HEPES buffer ($pK_a = 7.5$) are shown in Figure 7. Analogous data (Figures S4−S8 of Supporting Information) were collected at pH 7.4 in 20 mM PIPES buffer ($pK_a = 6.8$) and in 100 or 500 mM Tris buffer ($pK_a = 8.1$), where a higher concentration was required to provide sufficient excess of the basic form that binds metal ions. Table 2 indicates the average best-fit K_{ITC} and ΔH_{ITC}

parameters from at least two and typically three or more reproducible data sets.

The binding stoichiometry, n, is also a fit parameter with the one-site and competition binding models. Although its fit error is generally small (Figure 7 caption), the experimental error for n is considerably larger, as it depends on the accuracy of two concentrations and several injection volumes. While n is expected to be 1.0 for these peptides, cysteines are susceptible to oxidation, which suppresses metal binding and lowers the metal-binding stoichiometry. The DTNB assay was used to quantify free thiols and thereby the concentration of peptide that is used to determine the n fit value. However, this gives an upper limit by overestimating the amount of peptide with all of its cysteines reduced. Since the loss of one Cys significantly lowers the metal affinity,[50] n is generally somewhat lower than 1.0, which is based on the free thiol assay. The anaerobic environment around the calorimeter prevents oxidation during the >2 h of data collection, and a noisy drifting baseline that is characteristic of sample oxidation during a titration was not observed, nor was weak Zn^{2+} binding to partially oxidized peptide.

Table 2 also contains ITC results for Co^{2+} binding to Sp1-3 and MyT1-2 and for Zn^{2+} binding by subsequent displacement of the bound Co^{2+} (Figures S9 and S10 of Supporting Information). These data were analyzed with a competition binding model[43] that accounts for the increasing concentration of the displaced Co^{2+}.

As indicated in eq 4, which is Hess's law for Zn^{2+} binding to these peptides, the buffer protonation enthalpy ($\Delta H^{\circ}_{buffH^+}$)

$$\Delta H_{ITC} = -\Delta H^{\circ}_{Zn-buff} - n_{H^+}\Delta H^{\circ}_{pepH^+} + n_{H^+}\Delta H^{\circ}_{buffH^+} + \Delta H^{\circ}_{Zn-pep} \quad (4)$$
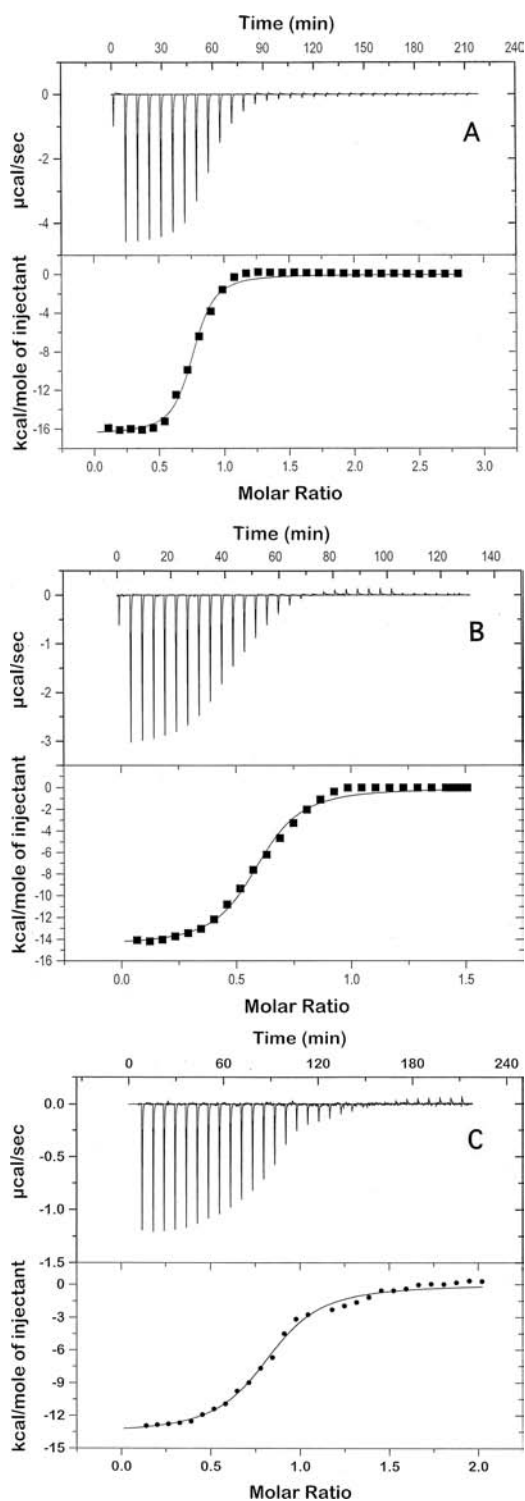
Figure 7. Representative 25 °C ITC binding isotherms and best fits for Zn^{2+} titrations into (A) Sp1-3 ($n = 0.73 \pm 0.01$, $K_{ITC} = (1.5 \pm 0.2) \times 10^6$, $\Delta H_{ITC} = -16.5 \pm 0.2$ kcal/mol), (B) MyT1-2 ($n = 0.58 \pm 0.01$, $K_{ITC} = (7.2 \pm 0.8) \times 10^5$, $\Delta H_{ITC} = -14.6 \pm 0.2$ kcal/mol), and (C) GR-2 ($n = 0.82 \pm 0.01$, $K_{ITC} = (1.0 \pm 0.1) \times 10^6$, $\Delta H_{ITC} = -13.7 \pm 0.2$ kcal/mol) in 20 mM HEPES buffer, pH 7.4, with 100 mM NaCl.

contributes to the experimental enthalpy, and the buffer dependence of ΔH_{ITC} can be used to quantify the number of protons (n_{H^+}) that are transferred (typically displaced) upon Zn^{2+} binding.[51,52] This analysis, however, must also account for the enthalpy of the metal−buffer interaction, which varies with

the buffer ($\Delta H°_{Zn\text{-}buff} = -0.29$, $+0.22$, and -2.45 kcal/mol for HEPES, PIPES, and Tris, respectively).[53] Therefore, eq 5 is the

$$(\Delta H_{ITC} + \Delta H°_{Zn\text{-}biff})$$
$$= n_{H^+}\Delta H°_{buffH^+} + (\Delta H°_{Zn\text{-}pep} - n_{H^+}\Delta H°_{pepH^+}) \qquad (5)$$

appropriate linear relationship, which indicates that a plot of $(\Delta H_{ITC} + \Delta H°_{Zn\text{-}buff})$ versus $\Delta H°_{buffH^+}$ has a slope corresponding to n_{H^+}. This analysis of the ITC data for Zn^{2+} binding to the peptides in three buffers with significantly different protonation enthalpies ($\Delta H°_{buffH^+} = -5.12$, -2.78, and -11.36 kcal/mol for HEPES, PIPES, and Tris, respectively)[54] indicates that 2.3 ± 0.3, 2.9 ± 0.2, and 4.1 ± 0.4 protons are displaced at pH 7.4 when Zn^{2+} binds to Sp1-3, MyT1-2, and GR-2, respectively (Figure S11 of Supporting Information). As expected, these values are close to the number of Zn-binding Cys residues (two, three, and four) that are predominantly protonated at this pH. Based on the pK_a's of the four Zn-binding residues of Sp1-3 determined by NMR, a simple Henderson−Hasselbalch analysis predicts that 1.8 ± 0.2 protons would be displaced upon Zn^{2+} binding to Sp1-3 at pH 7.4, which is within experimental error of the value determined from the ITC data. Finally, the intercept of the $(\Delta H_{ITC} + \Delta H°_{Zn\text{-}buff})$ versus $\Delta H°_{buffH^+}$ plot (eq 5) indicates the net enthalpy for Zn^{2+} binding and H^+ displacement from the peptide, $\Delta H°_{Zn\text{-}pep} - n_{H^+}\Delta H°_{pepH^+}$. These values are -5 ± 2, -2 ± 2, and $+10 \pm 4$ kcal/mol for Sp1-3, MyT1-2, and GR-2, respectively.

Since the buffer can have a significant effect on calorimetric data involving metal ions, the contributions of metal−buffer interaction ($\log K_{Zn\text{-}Buff} = 3.38$, 3.07, and 3.56 (β_2) for HEPES, PIPES, and Tris, respectively)[53] to the experimental binding constant (K_{ITC}), and the contributions of the metal−buffer enthalpy ($\Delta H°_{Zn\text{-}buff}$) and buffer protonation enthalpy ($n_{H^+}\Delta H°_{buffH^+}$) to the experimental binding enthalpy (ΔH_{ITC}) have been subtracted from the data in Table 2, as described recently.[27] Table 3 contains the corresponding buffer-independent calorimetric values at pH 7.4 and 25 °C.

Finally, the buffer-independent binding constants and binding enthalpies were used to determine the binding thermodynamics at pH 7.4 from standard relationships. Table 4 contains these values for data collected in the three buffers, as well as the average binding thermodynamics. The entropy is indicated with values of $-T\Delta S°$ at 298 K, which has the same units and sign as $\Delta H°$ for direct comparison of enthalpic and entropic contributions to $\Delta G°$.

■ DISCUSSION

Many transcription factor proteins, including those with tandem arrays of zinc fingers or other DNA-binding motifs, are stabilized by one or more Zn^{2+} ions binding to Cys and His residues. Thus, the active form of these proteins depends on the thermodynamic contributions of Zn^{2+} coordination. Further, any competition by other (toxic) metal ions for these binding sites will also depend on the Zn^{2+}-binding thermodynamics.

Previous studies have used ITC to quantify the thermodynamics of Zn^{2+} binding to relevant peptides, and two have studied this in considerable detail. Blaise and Berg measured the binding enthalpy and determined the thermodynamics of Zn^{2+} and Co^{2+} binding to the optimized consensus peptide, CP-1,[23] which has recently been shown to have the highest affinity for Zn^{2+} of the classical zinc fingers.[55] More recently,

Table 2. Average Best-Fit Parameters for ITC Data from Zn^{2+} and Co^{2+} Binding to Sp1-3, MyT1-2, and GR-2 in HEPES, PIPES, and Tris Buffers at pH 7.4 and 25 °C

		Sp1-3 (C_2H_2)	MyT1-2 (C_2HC)	GR-2 (C_4)
Zn^{2+}	K_{ITC}	$(1.2 \pm 0.3) \times 10^6$	$(7 \pm 1) \times 10^5$	$(4 \pm 3) \times 10^6$
(20 mM HEPES)	$\Delta H_{ITC}{}^a$	-16.5 ± 0.2	-14.5 ± 0.3	-10 ± 2
Zn^{2+}	K_{ITC}	$(6 \pm 4) \times 10^6$	$(8 \pm 2) \times 10^5$	
(20 mM PIPES)	$\Delta H_{ITC}{}^a$	-12 ± 1	-11.5 ± 0.5	
Zn^{2+}	K_{ITC}	$(1.1 \pm 0.3) \times 10^6$	$(4.6 \pm 0.5) \times 10^{5\ b}$	3×10^5
(500 mM Tris)	$\Delta H_{ITC}{}^a$	-29 ± 1	-33 ± 1^b	-34
Co^{2+}	K_{ITC}	$(2.2 \pm 0.8) \times 10^{5\ c}$	$(3.9 \pm 0.5) \times 10^{5\ d}$	
	$\Delta H_{ITC}{}^a$	-12 ± 1^c	-11 ± 2^d	
Zn^{2+}	K_{ITC}	$(4 \pm 2) \times 10^{6\ c}$	$(3.3 \pm 0.5) \times 10^{7\ d}$	
(indirect)	$\Delta H_{ITC}{}^a$	-25 ± 1^c	-12.5 ± 0.2^d	

[a] In kcal/mol. [b] 100 mM Tris. [c] 500 mM Tris. [d] 20 mM HEPES.

Table 3. Average Buffer-Independent Binding Constants and Enthalpies from ITC Data for Zn^{2+} and Co^{2+} Binding to Sp1-3, MyT1-2, and GR-2 in the Indicated Buffer at pH 7.4 and 25 °C

		Sp1-3 (C_2H_2)	MyT1-2 (C_2HC)	GR-2 (C_4)
Zn^{2+}	K	$(3 \pm 1) \times 10^7$	$(1.6 \pm 0.3) \times 10^7$	$(9 \pm 6) \times 10^7$
(20 mM HEPES)	$\Delta H°\,^a$	-5.0 ± 0.5	$+0.1 \pm 0.5$	$+10 \pm 2$
Zn^{2+}	K	$(1.2 \pm 0.8) \times 10^8$	$(1.6 \pm 0.4) \times 10^7$	
(20 mM PIPES)	$\Delta H°\,^a$	-5.4 ± 0.5	-3.2 ± 0.2	
Zn^{2+}	K	$(4 \pm 1) \times 10^7$	$(2.3 \pm 0.3) \times 10^{6\ b}$	1×10^7
(500 mM Tris)	$\Delta H°\,^a$	-5.3 ± 0.5	-2.5 ± 0.1^b	$+10$
	K_{ave}	$(6 \pm 3) \times 10^7$	$(1.1 \pm 0.8) \times 10^7$	$(5 \pm 4) \times 10^7$
Co^{2+}	K	$(1.2 \pm 0.4) \times 10^{6\ c}$	$(6.6 \pm 0.8) \times 10^{6\ d}$	
	$\Delta H°\,^a$	$+12 \pm 1^c$	$+4 \pm 1^d$	
Zn^{2+}	K	$(1.7 \pm 0.9) \times 10^{8\ c}$	$(8 \pm 1) \times 10^{8\ d}$	
(indirect)	$\Delta H°\,^a$	-1.3 ± 0.1^c	$+2.1 \pm 0.3^d$	

[a] In kcal/mol. [b] 100 mM Tris. [c] 500 mM Tris. [d] 20 mM HEPES.

Gibney and co-workers have investigated the thermodynamics of Zn^{2+} binding to a designed set of short glycine-rich peptides that vary the number of Cys and His ligands.[25]

We have studied three peptides that correspond to naturally occurring Zn-binding sequences, focusing mainly on a structurally characterized classical zinc finger with Cys_2His_2 coordination, Sp1-3. We also consider a zinc finger with $Cys_2HisCys$ coordination, MyT1-2, but lacking Zn-stabilized secondary structure. The absence of a classical $\beta\beta\alpha$ zinc finger structure for this and related sequences has been attributed to a higher prevalence of proline and glycine residues,[31] a slightly different spacing of the Cys and His residues and the absence of conserved hydrophobic residues.[34] We find that the residues in this sequence have a lower propensity to form α helical and β sheet secondary structures than do the residues at corresponding positions of several classical zinc fingers (Table S1 of Supporting Information). Finally, we have studied a Zn-binding sequence that coordinates the metal ion with four cysteines, GR-2, but little Zn-stabilized secondary structure. This study allows us to compare previous thermodynamic results on non-

native sequences to results on these native Zn-binding sequences.

Our recently summarized insight about factors that affect the collection and analysis of ITC data involving metal ions has guided this research.[27] A major consideration is the buffer, both its interaction with the metal ion and its role in coupled proton transfer equilibria. This is reflected in the range of experimental enthalpy values for Zn^{2+} binding to the peptides in three different buffers (Table 2). Accurate subtraction of these buffer effects in subsequent data analysis is confirmed by the similar thermodynamic values obtained for Sp1-3 in the three buffers (Table 4). Although the thermodynamics of Zn^{2+} binding to MyT1-2 in these buffers are not as consistent, Zn^{2+} coordination to this peptide stabilizes little secondary structure and may involve a second conserved histidine, which could be affected by the identity of the buffer. The GR-2 peptide has five Cys residues and is quite susceptible to oxidation, as is its ER-2 analogue,[13] providing significant challenges for spectral and ITC measurements of its Zn-binding properties. While larger errors are associated with data for this peptide, its

Table 4. Thermodynamics^a of Zn^{2+} Binding to Sp1-3, MyT1-2, and GR-2 in the Indicated Buffers at pH 7.4 and 298 K

		Sp1-3 (C$_2$H$_2$)	MyT1-2 (C$_2$HC)	GR-2 (C$_4$)
Zn^{2+}	$\Delta G°$	−10.2	−9.8	−10.8
(20 mM HEPES)	$\Delta H°$	−5.0 ± 0.5	+0.1 ± 0.5	+10 ± 2
	$-T\Delta S°$	−5.2	−9.9	−20.8
Zn^{2+}	$\Delta G°$	−11.0	−9.8	
(20 mM PIPES)	$\Delta H°$	−5.4 ± 0.5	−3.2 ± 0.2	
	$-T\Delta S°$	−5.6	−6.6	
Zn^{2+}	$\Delta G°$	−10.4	−8.7^b	−9.5
(500 mM Tris)	$\Delta H°$	−5.3 ± 0.5	−2.5 ± 0.1^b	+10
	$-T\Delta S°$	−5.1	−6.2^b	−19.5
average	$\Delta G°$	−10.5 ± 0.3	−9.4 ± 0.4	−10 ± 1
	$\Delta H°$	−5.2 ± 0.2	−2 ± 1	+10 ± 2
	$-T\Delta S°$	−5.3 ± 0.2	−7.5 ± 1.5	−20 ± 2
Co^{2+}	$\Delta G°$	−8.3^c	−9.3^d	
	$\Delta H°$	+12 ± 1^c	+4 ± 1^d	
	$-T\Delta S°$	−20^c	−13.3^d	
Zn^{2+}	$\Delta G°$	−11.2^c	−12.1^d	
(indirect)	$\Delta H°$	−1.3 ± 0.1^c	+2.1 ± 0.3^d	
	$-T\Delta S°$	−9.9^c	−14.2^d	

^{a}In kcal/mol. ^{b}100 mM Tris. ^{c}500 mM Tris. ^{d}20 mM HEPES.

thermodynamic values are quantitatively different from those of the other two peptides.

Proton Competition. The competition between metal ions and protons for basic ligands in aqueous solution is a well-known phenomenon that has significant consequences for calorimetric measurements. Not only does it lead to a pH-dependence of the experimental binding constant, but it also contributes to the experimental binding enthalpy. Protons displaced by a metal will bind to the buffer, and it is crucial that they are quantified so the associated buffer protonation enthalpy can be subtracted to determine the buffer-independent metal binding enthalpy. The number of displaced protons can be determined from the pH dependence of the metal binding constant or it can be deduced at a given pH from the pK_a's of the metal-binding residues. It can also be found by collecting ITC data in different buffers and determining the contribution of the buffer protonation enthalpy to the experimental enthalpy. However, accurate quantification of displaced protons by this ITC method also requires that the enthalpy of the interaction of the metal with the different buffers be included in the analysis.

We have used two methods to ensure accurate accounting of proton transfer equilibria in the analysis of ITC data. First, NMR signals of the Zn-coordinating residues of Sp1-3 have been assigned and their pH dependence has been monitored to experimentally determine their pK_a's (Table 1), which were then used to estimate the number of protons that are displaced upon Zn^{2+} binding at pH 7.4. Second, the ITC method has been used with three different buffers at pH 7.4. The number of Zn-displaced protons determined by this latter method is within experimental error of the number estimated with the NMR-derived pK_a's. Therefore, we have used the ITC method to determine the number of protons displaced by Zn^{2+} binding

to MyT1-2 and GR-2, and find these values to be close to the number of Cys ligands of each peptide.

Previous ITC studies of Zn^{2+} binding to peptides have determined the number of protons that are displaced. In one case the number was estimated from the pH-dependence of the Co^{2+}-binding constant of the peptide.[19] In the thermodynamic study of CP-1, the number was determined by the ITC method at pH 7.0 to be 1.1 protons,[23] which is unexpectedly low. Recently, the pK_a's of the Zn-binding residues of CP-1 have been determined by NMR measurements[55] and, based on these values, the Zn^{2+} should displace 2.1 protons at pH 7.0. Gibney and co-workers used both the ITC method and the relevant pK_a's, determined with potentiometric titrations, to estimate the number of displaced protons for their synthetic GGG peptides, and the two methods were in reasonable agreement.[25] In neither of these cases, however, was the metal-buffer enthalpy subtracted in the analysis of the ITC data, though for some buffers this value may be smaller than the error in the experimental enthalpy.

These measurements of the number of Zn-displaced protons are important for another reason. There is evidence from mass spectral data[56−58] and computational studies[59,60] that Zn^{2+} binding to peptides such as these can result in Cys thiol ligation without deprotonation. This motivated us to use ITC and NMR measurements in aqueous solution to determine whether Cys thiolates coordinate the Zn^{2+} ion when it is bound to the classical Sp1-3 zinc finger peptide at pH 7.4. The concern here is that mass spectral measurements may not accurately reflect the solution coordination chemistry.

Colorimetric−Calorimetric Comparison. A common method to determine the affinity of peptides and proteins for Zn^{2+} is based on its displacement of the chemically similar Co^{2+} ion and loss of the ligand field or charge transfer spectral features associated with Co^{2+} bound at the Zn^{2+} site. With a

Table 5. Buffer-Independent Zn^{2+} Affinities of ~30-Residue Zinc Finger Peptides

peptide	pH	buffer	method	K	$\log K$	ref
			Cys_2His_2			
CP-1 $(C_2H_2)^a$	7.0	50 mM MOPS, 100 mM phosphate	CD (ligand competition)	8×10^{14}	14.9	55
WT1-3^b	6.5	50 mM HEPES	ITC	7×10^9	9.8	24
TFIIIA-2^c	7.0	20 mM HEPES	Absorption (Co^{2+} displacement)	3×10^9	9.5	62
Sp1-3	7.0	50 mM HEPES	Absorption (Co^{2+} displacement)	$(4 \pm 1) \times 10^9$	9.6	30, d
Sp1-3	7.4	20 mM HEPES; 20 mM PIPES; 500 mM Tris	ITC	$(6 \pm 3) \times 10^7$	7.8	d
Sp1-3	7.4	500 mM Tris	ITC (Co^{2+} displacement)	$(1.7 \pm 0.9) \times 10^8$	8.2	d
ZFY-6^e	6.5	50 mM HEPES	ITC	4×10^7	7.6	20
Ant-F^f	7.5	10 mM (?) Tris	Absorption (Co^{2+} displacement)	8×10^7	7.9	63
			$Cys_2HisCys$			
CP-1 $(C_2HC)^a$	7.0	50 mM MOPS, 100 mM phosphate	CD (ligand competition)	1×10^{15}	15.0	55
NZF-13^g	7.0	100 mM HEPES	Absorption (Co^{2+} displacement)	3×10^{10}	10.5	33
MyT1-2	7.0	50 mM HEPES	Absorption (Co^{2+} displacement)	$(1.0 \pm 0.3) \times 10^9$	9.0	d
MyT1-2	7.4	20 mM HEPES; 20 mM PIPES; 100 mM Tris	ITC	$(1.1 \pm 0.8) \times 10^7$	7.0	d
MyT1-2	7.4	20 mM HEPES	ITC (Co^{2+} displacement)	$(8 \pm 1) \times 10^8$	8.9	d
			Cys_4			
CP-1 $(C_4)^a$	7.0	50 mM MOPS, 100 mM phosphate	CD (ligand competition)	4×10^{12}	12.6	55
XPA^h	7.4	50 mM phosphate	Fluorescence (Ni^{2+} competition)	$(6 \pm 4) \times 10^9$	9.8	64
GR-2	7.4	20 mM HEPES; 500 mM Tris	ITC	$(5 \pm 4) \times 10^7$	7.7	d

^{a}Consensus zinc finger peptide. ^{b}Peptide corresponding to the third zinc finger of the tumor suppressor protein associated with Wilm's tumor. ^{c}Peptide corresponding to the second zinc finger of TFIIIA. ^{d}This study. ^{e}Peptide corresponding to the sixth zinc finger of the human male-associated ZFY protein. ^{f}Peptide based on a two Cys variant of a sequence from Antennapedia homeodomain. ^{g}Peptide corresponding to the third zinc finger of NZF-1. ^{h}Peptide corresponding to the Zn^{2+}-binding sequence of the nucleotide excision repair protein XPA.

known value for K_{Co}, which is typically determined from a direct spectral titration, the value of K_{Zn} is then obtained from $K_{competition}$ determined from the displacement spectral titration.

Recently, Sénèque and Latour have evaluated spectrophotometric measurements of Co^{2+} and Zn^{2+} binding to zinc finger peptides, redetermined the Zn^{2+} affinities of the CP-1 peptides, and recommended procedures to obtain accurate stability constants,[55] which are discussed more generally by Xiao and Wedd.[61] Specifically, titrations with a fractional saturation that is too high lead to inaccurate values for the stability constant and require measurements with a competing ligand. These new results[55] for CP-1 indicate that its Zn^{2+} affinity is 2−3 orders of magnitude higher than previously reported.[45]

While the fractional saturation is clearly a crucial consideration, we find that buffer complexes with metal ions have sometimes been neglected. For example, the original spectral measurements of Co^{2+} binding to TFIIIA-2[62] and CP-1(C_4)[45] were done in HEPES buffer, for which we have found $\log K_{Co\text{-HEPES}} = 3.25$. Accounting for this competing interaction[27] increases $\log K_{Co}$ for CP-1(C_4) by 1.64, which is ~70% of the discrepancy between its originally reported affinity and the recently reported value from ligand competition binding.[55] The Zn^{2+} affinities determined subsequently by Co^{2+} displacement would then be higher by this amount.

Since we have carefully accounted for metal-buffer interaction in our ITC and spectral measurements, comparison with other measurements requires a similar accounting for this interaction in determining the Zn^{2+} affinity. Table 5 compiles the binding constants of several ~30 residue zinc finger peptides obtained with different methods. The reported values have been corrected for buffer complexes with Zn^{2+} or the Co^{2+} that it displaces, when this interaction appears to have been neglected. The Zn^{2+} affinities of ~30 residue native zinc finger sequences are found, depending on the pH, within a range of about 3 orders of magnitude, ~10^7 to ~10^{10} ($K_d \approx 100$ nM to 100 pM). The optimized CP-1 peptides are noted for their

significantly higher Zn^{2+} affinities, the thermodynamic basis of which is discussed below.

For comparison to previous studies of CP-1[45] and NZF-13,[33] the Co^{2+} and Zn^{2+} affinities of Sp1-3 and MyT1-2 were determined by spectral titration under similar conditions (pH 7.0, HEPES buffer). After accounting for buffer competition, we find K_{Co} and K_{Zn} values for Sp1-3 that are within the range of values reported for other naturally occurring $\beta\beta\alpha$ classical zinc finger peptides[25] and significantly lower than both the earlier[45] and the more recent[55] values for CP-1. The spectral data for Co^{2+} binding to MyT1-2 do not exceed the fractional saturation limit, and the value of K_{Co} obtained from these data is consistent with that found for its homologue NZF-13.[33]

ITC data have a similar fractional saturation constraint, which is evaluated by the so-called c window, where $c = K[\text{macromolecule}]$ and $5 < c < 500$ sets the limits over which an accurate stability constant can be determined for 1:1 binding. Due to this limit, Blaise and Berg were unable to determine K_{Co} or K_{Zn} for CP-1 from their ITC data,[23] except for Co^{2+} binding at pH ≤ 6.3, and relied on stability constants (free energies) from spectral titrations.[45] The ITC data for Zn^{2+} binding to Sp1-3, MyT1-2, and GR-2 at pH 7.4 are all within the c window and, after accounting for metal-buffer interaction, provide accurate values for K_{Co} and K_{Zn} at this pH.

The Co^{2+}- and Zn^{2+}-binding constants obtained from spectral titrations can be compared to those obtained from calorimetric measurements of direct Co^{2+} and Zn^{2+} titrations and indirect titrations involving Zn^{2+} displacement of Co^{2+}, which mimics the spectral Zn^{2+} measurement. The K_{Co} and K_{Zn} values for Sp1-3 from direct ITC titrations are about an order of magnitude lower than those from spectral data. Two factors appear to contribute to this discrepancy. First, the spectral titration data[30] for Co^{2+} binding to Sp1-3 may exceed the fractional saturation limit, introducing uncertainty in K_{Co} and K_{Zn} obtained from analysis of these data. Second, the spectral data were obtained at a somewhat lower pH, which may affect

10414

dx.doi.org/10.1021/ja211417g | *J. Am. Chem. Soc.* 2012, 134, 10405−10418

Table 6. Thermodynamics of Zn^{2+} Binding to Peptides Containing Cys and His Residues at 298 K

peptide[a]	# aa's	pH	ΔG° [b]	ΔH° [b]	$-T\Delta S^{\circ}$ [b]	ΔS° [c]	n_{H+} [d]	$\Delta H^{\circ}_{Zn\text{-}pep}$ [e]
				Cys$_2$His$_2$				
Sp1-3	27	7.4	−10.5 ± 0.3	−5.2 ± 0.2	−5.3 ± 0.2	+17	2.3 ± 0.3	−25
CP-1	26	7.0	−20.3[f]	−21.1 ± 1.0[g]	+0.8 ± 1.0	−3	1.1[g]	−30
WT1-3	29	6.5	−13.4 ± 0.1[h]	−7.8 ± 0.4[i]	−5.6 ± 0.4	+19	(2.7)	−30
ZFY-6	30	6.5	−10.4[h]	+4.0 ± 0.1[i]	−14.4 ± 0.1	+48	(2.7)	−19
GGG-H$_2$C$_2$[j]	16	7.4	−16.3	−0.1	−16.2	+54	2.2	−19
GGG-H$_2$C$_2$[j]	16	7.0	−14.0	+3.3	−17.3	+58	2.5	−18
				Cys$_2$HisCys				
MyT1-2	29	7.4	−9.4 ± 0.4	−2 ± 1	−7.5 ± 1.5	+25	2.9 ± 0.2	−27
NC-1[k]	18	7.0	−20	−6.5	−13.5	+45	3	−32
NCp7-N[l]	18	7.5	−18.4 ± 0.1	−8.1 ± 0.7	−10.3 ± 0.7	+35		
NCp7-C[l]	18	7.5	−17.7 ± 0.1	−8.4 ± 0.2	−9.3 ± 0.2	+32		
GGG-HC$_3$[j]	16	7.4	−17.3	+1.0	−18.3	+61	2.9	−24
GGG-HC$_3$[j]	16	7.0	−15.0	+3.7	−18.7	+63	3.2	−24
				Cys$_4$				
GR-2	31	7.4	−10 ± 1	+10 ± 2	−20 ± 2	+70	4.1 ± 0.4	−25
GGG-C$_4$[j]	16	7.4	−17.4	+5.6	−23.0	+77	3.6	−25

[a]See Table 5 for description of some peptides. [b]In kcal/mol. [c]In cal/(mol K). [d]Protons displaced upon Zn^{2+} binding at the indicated pH. [e]See the text. [f]Ref 55. [g]Ref 23. [h]Zn^{2+}−buffer interaction removed. [i]Enthalpies of Zn^{2+}−buffer interaction and buffer protonation removed from the experimental binding enthalpy (latter estimated from Cys and His pK_a's of 8.2 and 6.2, respectively, determined for Sp1-3 with NMR). [j]Gly-rich peptide with four Zn-binding residues.[25] [k]Peptide corresponding to the N-terminal Zn-binding sequence of the HIV-1 nucleocapsid binding protein.[19] [l]Peptides corresponding to the N- and C-terminal Zn-binding sequences of the HIV-1 nucleocapsid protein (ΔH° from van't Hoff analysis of the temperature dependence of K).[65]

the binding constants due to the many charged Sp1-3 residues in this pH range. However, the K_{Zn} values determined from both direct and indirect (Co^{2+} displacement) ITC measurements are the same within error, indicating an internal consistency of the ITC data and analysis at pH 7.4. For MyT1-2, similar values are obtained for K_{Co} from direct spectral and direct ITC data, and for K_{Zn} from indirect spectral and indirect ITC data. However, the value of K_{Zn} from the direct ITC data is smaller than that obtained from the indirect (Co^{2+} displacement) titration. For this peptide, the additional conserved His residue and lack of metal-stabilized secondary structure may differentially affect the Co^{2+} and Zn^{2+} coordination, which could affect the indirect spectral and indirect ITC values for K_{Zn}.

Enthalpy and Entropy. A major goal of this study was to quantify the enthalpic and entropic contributions of Zn^{2+} binding to these naturally occurring sequences that provide a range of ligands (Cys$_2$His$_2$, Cys$_2$HisCys, Cys$_4$) and peptide secondary structure. Table 4 summarizes the Zn^{2+}-binding thermodynamics of these three peptides, and Table 6 compares these results to those reported, or estimated, from relevant peptides. These include the optimized and well-studied CP-1 zinc finger developed by Berg,[23] two naturally occurring zinc fingers studied by Weiss and co-workers,[21,24] three peptides corresponding to the Zn-binding sequences of the HIV-1 nucleocapsid protein,[19,65] and three short Gly-rich peptides designed and studied by Gibney and co-workers.[25] These last three provide useful comparisons, as it has been suggested that their Zn-binding thermodynamics should be dominated by the metal coordination. The following observations can be made about the data in Table 6.

Zinc binding to the classical zinc finger Sp1-3 is both enthalpically and entropically favored. In comparison, the high Zn^{2+} affinity of CP-1 is due to a very favorable enthalpy of binding but negligible entropic contributions. This is consistent with an optimized protein structure that contributes to the favorable binding enthalpy but also provides a larger protein entropic penalty (vide infra) that cancels favorable entropic contributions (e.g., desolvation, proton displacement). Estimates of the Zn^{2+}-binding thermodynamics of two other native $\beta\beta\alpha$ zinc fingers, WT1-3 and ZFY-6, at pH 6.5 indicate a favorable binding entropy, though both the enthalpy and entropy of binding appear to depend on other factors, such as the identity and position of other residues. In particular, ZFY-6 is representative of so-called aromatic swap zinc fingers, where one of the conserved hydrophobic residues is in an alternate position.[20,21] This may affect the enthalpy and entropy of formation of its Zn-stabilized structure, which are 12 kcal/mol less favorable and 9 kcal/mol more favorable, respectively, than the values for WT1-3 (Table 6).

The three naturally occurring Zn-binding sequences with Cys$_2$His$_2$, Cys$_2$HisCys, and Cys$_4$ coordination studied here have a similar affinity for Zn^{2+}, but this masks very different enthalpic and entropic contributions to the binding free energy. As more cysteines are included in the Zn^{2+} coordination, the enthalpy of binding becomes less favorable while the entropy of binding becomes more favorable, to the point where Cys$_4$ ligation is entropically driven with an enthalpic penalty. We attribute this correlation to an increasing contribution from the enthalpy required to deprotonate the Cys thiols but an entropic gain from lost protons. Gibney and co-workers found the same trend with their GGG peptides (Table 6) and drew a similar conclusion.[25]

To test this explanation, we have estimated the enthalpy of Zn^{2+} binding to Sp1-3, MyT1-2 and GR-2 with deprotonated Cys residues, designated $\Delta H^{\circ}_{Zn\text{-}pep}$ (Table 6). Making the approximation that Zn^{2+} displaces only protons from Cys residues at pH 7.4, ΔH°_{pepH+} in eqs 4 and 5 is replaced by ΔH°_{CysH} (+8.5 kcal/mol), as shown by eq 6.

$$\Delta H^{\circ} = \Delta H^{\circ}_{Zn\text{-}pep} - n_{H+}\Delta H^{\circ}_{CysH} \qquad (6)$$

The $\Delta H°_{\text{Zn-pep}}$ values for these three peptides, −25, −27, and −25, respectively, are very similar, indicating that differences in their total binding enthalpy at pH 7.4 are predominantly due to the enthalpic contribution from Cys thiol deprotonation. The similar $\Delta H°_{\text{Zn-pep}}$ values also indicate there are no significant differences in protein contributions to the binding enthalpy among these peptides, even though they have different amounts of Zn-stabilized secondary structure. Similar values of $\Delta H°_{\text{Zn-pep}}$ are also found for other peptides (Table 6), suggesting this may be a common feature of tetrahedral Zn^{2+} coordination.

The entropic contribution from protons displaced by Zn^{2+} is harder to estimate, but the value of $-T\Delta S°$ for Sp1-3, MyT1-2, and GR-2 becomes increasingly negative as more protons are displaced, indicating this is a significant contribution to the binding entropy. A plot of the number of displaced protons versus $-T\Delta S°$ for the three peptides has a roughly linear correlation ($R = 0.98$), though the error associated with these values obviates any further insight.

Comparison of the Zn-binding thermodynamics of the four naturally occurring sequences with $Cys_2HisCys$ coordination (Table 6) indicates that the significantly higher Zn^{2+} affinity of the 18-residue peptides from the HIV-1 nucleocapsid protein is due to more favorable contributions from both the enthalpy and the entropy of binding. While the entropy advantage over MyT1-2 is consistent with the ∼40% shorter peptide length, the large difference in binding enthalpy suggests a more favorable Zn^{2+} coordination to the nucleocapsid peptide sequences and possibly some contributions from the other residues.

The similar free energy yet different enthalpy and entropy components for Zn^{2+} binding to Sp1-3, MyT1-2, and GR-2 is another example of enthalpy−entropy compensation (EEC). Gibney and co-workers also found that their three GGG peptides exhibit a Zn-binding EEC, which they showed graphically with a linear plot of $\Delta H°$ vs $-T\Delta S°$.[25] A similar linear relationship is found for the three peptides studied here and for the aromatic swapped zinc finger ZFY-6, which has a similar value of $\Delta G°$. However, this classical zinc finger with Cys_2His_2 coordination falls between MyT1-2 ($Cys_2HisCys$) and GR-2 (Cys_4) on the $\Delta H°$ vs $-T\Delta S°$ plot. While this is primarily due to the lower pH of the ZFY-6 data and the larger number of protons that are displaced by Zn^{2+}, it may also reflect the enthalpic and entropic consequences of the less common position of the Phe residue of this $\beta\beta\alpha$ zinc finger.[20,21]

Metal and Protein Contributions. The thermodynamics of metal ions binding to proteins and stabilizing protein structure involve contributions from both metal coordination and interactions among the protein residues. Results from this and other studies allow these contributions to be estimated for these Zn-binding peptides. This is accomplished with somewhat higher confidence for the binding enthalpy, which is measured directly by ITC, and two types of analysis provide estimates of the protein contributions.

The $\Delta H°_{\text{Zn-pep}}$ values (Table 5) quantify the enthalpy of Zn^{2+} binding to peptides with deprotonated Cys residues, and include both the Zn-ligand bond enthalpies (relative to the $Zn-H_2O$ bond enthalpy) and the remaining enthalpy associated with the peptide ($\Delta H°_{\text{peptide}}$), as indicated in eq 7, where n_{His} is the number of His ligands.

$$\Delta H°_{\text{Zn-pep}} = (4 - n_{\text{His}})\Delta H°_{\text{Zn-Cys}} + n_{\text{His}}\Delta H°_{\text{Zn-His}}$$
$$+ \Delta H°_{\text{peptide}} \quad\quad (7)$$

Since the Zn^{2+} coordination is known, its contributions can be estimated from the enthalpy of Zn−imidazole and Zn−thiolate bonds. Although the free energy of formation of the latter bond appears to be approximately 2 kcal/mol more favorable,[25] we estimate from ITC measurements of Zn^{2+} binding to the small Cys-rich protein metallothionein[66] and the small His-rich protein Hpn[67] that $\Delta H°$ for Zn^{2+} binding to a His imidazole and a Cys thiolate are both approximately −5 kcal/mol. Thus, the values of $\Delta H°_{\text{peptide}}$ for Sp1-3, MyT1-2, and GR-2 are approximately −5, −7, and −5 kcal/mol, respectively. This indicates that metal coordination and protein contributions to the binding enthalpy are fairly constant across this series and dominated by Zn^{2+} bonding to the amino acid side chains, in spite of the significant amount of Zn-stabilized secondary structure of Sp1-3, relative to the other two peptides.

The second approach uses the results of Gibney and co-workers,[25] who suggest that the thermodynamics of Zn^{2+} binding to their short Gly-rich peptides is predominantly due to the metal coordination. They have used this assumption to estimate the peptide contributions to the free energy of Zn^{2+} binding to several peptides (Table 5 in ref 25). We have subtracted the Zn-binding thermodynamics of the relevant GGG peptide from those of the peptides in this study and others in Table 6. The resulting thermodynamic values are reported in Table 7 and are suggested to be predominantly associated with the protein. The following observations can be made about the values in Table 7.

Table 7. Thermodynamics of Protein Contributions to Zn^{2+} Binding to Peptides With Cys and His Residues at 298 K

peptide[a]	# aa's	pH	$\Delta\Delta G°$ [b,c]	$\Delta\Delta H°$ [b,c]	$-T\Delta\Delta S°$ [b,c]	$\Delta\Delta S°$ [b,d]
			Cys_2His_2			
Sp1-3	27	7.4	+5.8	−5.1	+10.9	−37
CP-1	26	7.0	−6.3	−24.4	+18.1	−61
WT1-3[e]	29	6.5	+0.6	−11.1	+11.7	−39
ZFY-6[e]	30	6.5	+3.6	+0.7	+2.9	−10
			$Cys_2HisCys$			
MyT1-2	29	7.4	+7.9	−3	+10.8	−36
NC-1	18	7.0	−5	−10	+5	−18
NCp7-N	18	7.5	−1.1	−9.1	+8.0	−26
NCp7-C	18	7.5	−0.4	−9.4	+9.0	−29
			Cys_4			
GR-2	31	7.4	+7	+4	+3	−10

[a]See Tables 5 and 6 for designation of peptides. [b]Obtained by subtraction of the corresponding value for the analogous GGG peptide[25] from the value in Table 6. [c]In kcal/mol. [d]In cal/(mol K). [e]Subtraction of pH 7.0 $GGG-H_2C_2$ peptide data.

1. $\Delta\Delta G°$ ($\Delta G°_{\text{pep−GGG}}$). For the ∼30 residue peptides, except CP-1, protein contributions to the free energy are unfavorable, consistent with the lack of a stable peptide structure in the absence of Zn^{2+}; $\Delta\Delta G°$ is modestly favorable for the optimized CP-1, based on the new stability constant,[55] and the 18-residue nucleocapsid peptides at 25 °C. These results generally agree with those reported by Gibney and co-workers,[25] although some of the values in Table 7 are different because metal−buffer interactions have been subtracted.

2. $\Delta\Delta H°$ ($\Delta H°_{\text{pep-GGG}}$). The other residues of most of the peptides, and especially CP-1, provide a favorable enthalpic contribution, relative to the predominantly glycine residues in the GGG peptides. This may be associated with hydrogen-bonding, π-stacking, and other inter-residue bonding inter-

actions. For Sp1-3, studied here in most detail, the value of $\Delta\Delta H°$ is remarkably similar to the $\Delta H°_{peptide}$ value determined above. However, the $\Delta\Delta H°$ values for MyT1-2 and especially GR-2 are less favorable than the corresponding $\Delta H°_{peptide}$ value. Relative to the GGG peptide, Zn^{2+} binding and stabilization of GR-2 may have to overcome favorable inter-residue interactions in the metal-free peptide.

3. $-T\Delta\Delta S°$ ($-T\Delta S°_{pep-GGG}$). All peptides have an entropic penalty, consistent with Zn^{2+} curtailing conformational degrees of freedom. This is particularly true for CP-1, where an optimized protein structure would result in an even greater loss of conformational and/or dynamic entropy. There is even a notable entropic penalty for the nucleocapsid peptides that are only two residues longer than the GGG-HC$_3$ peptide. The entropic penalty does not correlate with the extent of secondary structure, as there is a large range for this value among the four peptides with a known $\beta\beta\alpha$ zinc finger structure. Further, this value is similar for Sp1-3 and MyT1-2, which have considerable and negligible secondary structure, respectively, while GR-2, which also has little secondary structure, has a lower value.

Thus, residues not involved in coordinating the metal can play a significant role in the thermodynamics of Zn^{2+} stabilization of these protein structures. This has been quantitatively measured for a specific aromatic residue in a comparative thermodynamic and structural analysis of variant zinc finger peptides by Weiss and co-workers.[20,21]

CONCLUSIONS

We have measured the thermodynamics of Zn^{2+} binding to three peptides that correspond to naturally occurring Zn-binding sequences with ligands that vary from Cys_2His_2 to $Cys_2HisCys$ to Cys_4 and different amounts of Zn-stabilized secondary structure. Using multiple data sets in different buffers and recent insight about ITC measurements involving metal ions, internally consistent thermodynamic values have been achieved for each peptide. Although all three peptides have a similar affinity for Zn^{2+}, compensating trends in the binding enthalpy and entropy correlate with Zn^{2+} coordination to an increasing number of Cys residues, which is explained by an enthalpic penalty to deprotonate the thiol(s) but an entropic gain from loss of the proton(s). The entropically driven binding of Zn^{2+} to Cys_4 sites makes the stability of this coordination more susceptible to factors such as pH, temperature and the surrounding dielectric. The metal and protein thermodynamic components have been determined and Zn^{2+} coordination to the Cys and His residues dominates, with negligible contribution from protein secondary structure. Comparison of the Zn-binding thermodynamics of four structurally similar $\beta\beta\alpha$ zinc finger peptides reveals that other residues can modulate the protein enthalpic and entropic contributions to the overall stability.

ASSOCIATED CONTENT

Ⓢ Supporting Information

Additional spectroscopic (absorption and CD) and calorimetric (ITC) data of Co^{2+} and Zn^{2+} binding to the peptides, enthalpy plots, and table of secondary structure propensity analysis. This material is available free of charge via the Internet at http://pubs.acs.org.

AUTHOR INFORMATION

Corresponding Author
dwilcox@dartmouth.edu

Present Addresses
$^{\parallel}$Department of Chemistry, University of New South Wales, Sydney 2052, Australia
$^{\perp}$Experimentalphysik IV, Universität Bayreuth, 95447 Bayreuth, Germany
$^{\otimes}$Department of Chemistry, East Carolina University, Greenville, NC 27858
$^{\nabla}$Coalition Against Major Diseases, Critical Path Institute, Tucson, AZ 85718

Notes
The authors declare no competing financial interest.

REFERENCES

(1) Hanas, J. S.; Hazuda, D. J.; Bogenhagen, D. F.; Wu, F. Y.-H.; Wu, C.-W. *J. Biol. Chem.* **1983**, *258*, 14120−14125.
(2) Miller, J.; McLachlan, A. D.; Klug, A. *EMBO J.* **1985**, *4*, 1609−1614.
(3) Brown, R. S.; Sander, C.; Argos, P. *FEBS Lett.* **1985**, *186*, 271−274.
(4) Frankel, A. D.; Berg, J. M.; Pabo, C. O. *Proc. Natl. Acad. Sci. U.S.A.* **1987**, *84*, 4841−4845.
(5) Parraga, G.; Horvath, S. J.; Eisen, A.; Taylor, W. E.; Hood, L.; Young, E. T.; Klevit, R. E. *Science* **1988**, *241*, 1489−1492.
(6) Lee, M. S.; Gippert, G. P.; Soman, K. V.; Case, D. A.; Wright, P. E. *Science* **1989**, *245*, 635−637.
(7) Krishna, S. S.; Majumdar, I.; Grishin, N. V. *Nucleic Acids Res.* **2003**, *31*, 532−550.
(8) Summers, M. F.; South, T. L.; Kim, B.; Hare, D. R. *Biochemistry* **1990**, *29*, 329−340.
(9) Freedman, L. P.; Luisi, B. F.; Korszun, Z. R.; Basavappa, R.; Sigler, P. B.; Yamamoto, K. R. *Nature* **1988**, *334*, 543−546.
(10) Härd, T.; Kellenbach, E.; Boelens, R.; Maler, B. A.; Dahlman, K.; Freedman, L. P.; Carlstedt-Duke, J.; Yamamoto, K. R.; Gustafson, J.-Å.; Kaptein, R. *Science* **1990**, *249*, 157−160.
(11) Luisi, B. F.; Xu, W. X.; Otwinowski, Z.; Freedman, L. P.; Yamamoto, K. R.; Sigler, P. B. *Nature* **1991**, *352*, 497−505.
(12) Archer, T. K.; Hager, G. L.; Omichinski, J. G. *Proc. Natl. Acad. Sci. U.S.A.* **1990**, *87*, 7560−7564.
(13) Whittal, R. M.; Benz, C. C.; Scott, G.; Semyonov, J.; Burlingame, A. L.; Baldwin, M. A. *Biochemistry* **2000**, *39*, 8406−8417.
(14) Zeng, J.; Heuchel, R.; Schaffner, W.; Kägi, J. H. R. *FEBS Lett.* **1991**, *279*, 310−312.
(15) Andrews, G. K. *Biometals* **2001**, *14*, 223−237.
(16) Sunderman, F. W., Jr.; Barber, A. M. *Ann. Clin. Lab. Sci.* **1988**, *18*, 267−288.
(17) Witkiewicz-Kucharczyk, A.; Bal, W. *Toxicol. Lett.* **2006**, *162*, 29−42.
(18) Wilcox, D. E. *Inorg. Chim. Acta* **2008**, *361*, 857−867.
(19) McLendon, G.; Hull, H.; Larkin, K.; Chang, W. *J. Biol. Inorg. Chem.* **1999**, *4*, 171−174.
(20) Lachenmann, M. J.; Ladbury, J. E.; Phillips, N. B.; Narayana, N.; Qian, X.; Weiss, M. A. *J. Mol. Biol.* **2002**, *316*, 969−989.

(21) Lachenmann, M. J.; Ladbury, J. E.; Qian, X.; Huang, K; Singh, R.; Weiss, M. A. *Protein Sci.* **2004**, *13*, 3115−3126.

(22) Krizek, B. A.; Amann, B. T.; Kilfoil, V. J.; Merkle, D. L.; Berg, J. M. *J. Am. Chem. Soc.* **1991**, *113*, 4518−4523.

(23) Blaise, C. A.; Berg, J. M. *Biochemistry* **2002**, *41*, 15068−15073.

(24) Lachenmann, M. J.; Ladbury, J. E.; Dong, J.; Huang, K.; Carey, P.; Weiss, M. A. *Biochemistry* **2004**, *43*, 13910−13925.

(25) Reddi, A. R.; Guzman, T. R.; Breece, R. M.; Tierney, D. L.; Gibney, B. R. *J. Am. Chem. Soc.* **2007**, *129*, 12815−12827.

(26) Zhang, Y.; Akilesh, S.; Wilcox, D. E. *Inorg. Chem.* **2000**, *39*, 3057−3064.

(27) Grossoehme, N. E.; Spuches, A. M.; Wilcox, D. E. *J. Biol. Inorg. Chem.* **2010**, *15*, 1183−1191.

(28) Kadonaga, J. T.; Carner, K. R.; Masiarz, F. R.; Tjian, R. *Cell* **1987**, *51*, 1079−1090.

(29) Narayan, V. A.; Kriwacki, R. W.; Caradonna, J. P. *J. Biol. Chem.* **1997**, *272*, 7801−7809.

(30) Posewitz, M. C.; Wilcox, D. E. *Chem. Res. Toxicol.* **1995**, *8*, 1020−1028.

(31) Kim, J. G.; Hudson, L. D. *Mol. Cell. Biol.* **1992**, *12*, 5632−5639.

(32) Jiang, Y.; Yu, V. C.; Buchholz, F.; O'Connell, S.; Rhodes, S. J.; Candeloro, C.; Xia, Y.-R.; Lusis, A. J.; Rosenfeld, M. G. *J. Biol. Chem.* **1996**, *271*, 10723−10730.

(33) Blaise, C. A.; Berg, J. M. *Inorg. Chem.* **2000**, *39*, 348−351.

(34) Berkovitz-Cymet, H. J.; Amann, B. T.; Berg, J. M. *Biochemistry* **2004**, *43*, 898−903.

(35) Gamsjaeger, R.; Swanton, M. K.; Kobus, F. J.; Lehtomaki, E.; Lowry, J. A.; Kwan, A. H.; Matthews, J. M.; Mackay, J. P. *J. Biol. Chem.* **2008**, *283*, 5158−5167.

(36) Jocelyn, P. C. *Methods Enzymol.* **1987**, *143*, 44−67.

(37) Binstead, R; Zuberbuhler, A. *SPECFIT Global Analysis System*, V3.0; Spectrum Software Associates: Marlborough, MA, 2000.

(38) Piotto, M.; Saudek, V.; Sklenář, V. *J. Biomol. NMR* **1992**, *2*, 661−665.

(39) Sklenář, V.; Piotto, M.; Leppik, R.; Saudek, V. *J. Magn. Reson. Ser. A* **1993**, *102*, 241−245.

(40) Braunschweiler, L.; Ernst, R. R. *J. Magn. Reson.* **1983**, *53*, 521−528.

(41) Bax, A.; Davis, D. G. *J. Magn. Reson.* **1985**, *65*, 355−360.

(42) Jenner, J.; Meier, B. H.; Bachmann, P.; Ernst, R. R. *J. Chem. Phys.* **1979**, *71*, 4546−4553.

(43) Sigurskjold, B. W. *Anal. Biochem.* **2000**, *277*, 260−266.

(44) Lever, A. B. P. *Inorganic Electronic Spectroscopy*, 2nd ed.; Elsevier: Amsterdam, 1984.

(45) Krizek, B. A.; Merkle, D. L.; Berg, J. M. *Inorg. Chem.* **1993**, *32*, 937−940.

(46) Bombarda, E.; Morellet, N.; Cherradi, H.; Spiess, B.; Bouaziz, S.; Grell, E.; Roques, B. P.; Mély, Y. *J. Mol. Biol.* **2001**, *310*, 659−672.

(47) Wüthrich, K. *NMR of Proteins and Nucleic Acids*; Wiley: New York, 1986.

(48) Dyson, H. J.; Tennant, L. L.; Holmgren, A. *Biochemistry* **1991**, *30*, 4262−4268.

(49) Creighton, T. E. *Proteins: Structures and Molecular Properties*, 2nd ed.; Freeman: New York, 1993.

(50) Merkle, D. L.; Schmidt, M. H.; Berg, J. M. *J. Am. Chem. Soc.* **1991**, *113*, 5450−5451.

(51) Doyle, M. L.; Louie, G.; Dal Monte, P. R.; Sokoloski, T. D. *Methods Enzymol.* **1995**, *259*, 183−194.

(52) Baker, B. M.; Murphy, K. P. *Biophys. Chem.* **1996**, *71*, 2049−2055.

(53) Grossoehme, N. E., Ph.D. thesis, Dartmouth College, 2007.

(54) NIST Standard Reference Database 46, 2003.

(55) Sénèque, O.; Latour, J.-M. *J. Am. Chem. Soc.* **2010**, *132*, 17760−17774.

(56) Fabris, D.; Zaia, J.; Hathout, Y.; Fenselau, C. *J. Am. Chem. Soc.* **1996**, *118*, 12242−12243.

(57) Fabris, D.; Hathout, Y.; Fenselau, C. *Inorg. Chem.* **1999**, *38*, 1322−1325.

(58) Larabee, J. L.; Hocker, J. R.; Hanas, J. S. *Arch. Biochem. Biophys.* **2005**, *434*, 139−149.

(59) Simonson, T.; Calimet, N. *Proteins: Struct., Funct. Genet.* **2002**, *49*, 37−48.

(60) Dudev, T.; Lim, C. *J. Am. Chem. Soc.* **2002**, *124*, 6759−6766.

(61) Xiao, Z.; Wedd, A. G. *Nat. Prod. Rept.* **2010**, *27*, 768−789.

(62) Berg, J. M.; Merkle, D. L. *J. Am. Chem. Soc.* **1989**, *111*, 3759−3761.

(63) Hori, Y.; Sugiura, Y. *J. Am. Chem. Soc.* **2002**, *124*, 9362−9363.

(64) Bal, W.; Schwerdtle, T.; Hartwig, A. *Chem. Res. Toxicol.* **2003**, *16*, 242−248.

(65) Mély, Y.; De Rocquigny, H.; Morellet, N.; Roques, B. P.; Gérard, D. *Biochemistry* **1996**, *35*, 5175−5182.

(66) Quinn, C. F., Ph.D. thesis, Dartmouth College, 2009.

(67) Zhang, Y., Ph.D. thesis, Dartmouth College, 2001.